Journal of Computational Electronics (2022) 21:431–444
https://doi.org/10.1007/s10825-022-01865-1

6G Rotman lens D-band beam-steering microstrip antenna

Uri Nissanov[1]

Received: 14 August 2021 / Accepted: 24 January 2022 / Published online: 15 February 2022

Abstract
This paper presents a design flowchart, design equations, and design of a D-band Rotman lens beam-steering microstrip array antenna at 110–145 GHz operating frequency. The initial design of the Rotman lens was done by Remcom Rotman lens designer (RLD) software. Then, the Rotman lens geometry was exported to a 3D full-wave analysis with the time-domain solver at the CST MWS simulator. In addition, state-of-the-art microstrip patches radiators were designed, embedded with the Rotman lens geometry, and optimized with the time-domain solver at the CST MWS simulator. Finally, the D-band Rotman lens beam-steering microstrip array antenna was also simulated for comparison with the frequency-domain solver at the CST MWS simulator, and a good agreement was achieved, which validated the proposed flowchart, design equations, and design of the beam-steering antenna. The proposed design can be a base for a large microstrip array with more significant gain and a wider beam-steering angle reported in the research. Thus, the D-band Rotman lens beam-steering microstrip array antenna can be a proper candidate for next-generation backhauling cellular communication at the sixth generation (6G).

Keywords D-band beam-steering antenna · Rotman lens designer (RLD) · Sixth generation (6G)

1 Introduction

D-band is a frequency range between 110 and 170 GHz, part of the millimeter-wave (mmWave) band. The increasing need to transmit the data rate beyond 10–100 gigabit per second (Gb/s) pushes transceivers to a higher-frequency range. As a result, D-band is now considered an alternative to optical fiber backhauling next-generation cellular communication networks beyond the fifth generation (B5G) or sixth generation (6G) [1, 2].

5G wireless communication technology is being installed worldwide, with multiple intelligent implementations being embedded. However, 5G specifications have not included the requirements of modern emerging technologies. These include terabit per second (Tb/s) data rate, high reliability, low latency, and high capacity [3, 4]. Researchers pay particular attention to 6G cellular communications to mitigate these challenging demands by enabling new applications and diverse technologies. In concepts of speed, 6G will use an upper frequency band than 5G to improve the data rate, which is predicted to be dozens of times faster than 5G. 6G will allow a hundred Gb/s to Tb/s links by using the high-spread spectrum and multi-band technique; In concepts of capacity, 6G will be able to be effective and connect up to 10^{12} devices certainly than the current 10^{9} cellular devices [5, 6]. So, 6G will become highly dense, and its capacity can be 100 times higher than that of 5G. In concepts of latency, 6G will be allowed latency of 1 ms or even lower down to 0.1 ms for radio latency [7].

The THz band (0.1–10 THz) experiences high propagation losses because of the resonance with water vapor and oxygen molecules at these frequencies. Therefore, there are frequency bands in the THz, such as 125–170 GHz and 190–320 GHz, where the attenuation is less than 100 dB/km, allowing short-range line-of-sight (LoS) cellular communication. On the other hand, the D-band predictable propagation loss is about 1 dB/km, so the D-band is a possible candidate for the next-generation 6G cellular communication [8, 9].

The 6G cellular communication demands considerable research and development in antenna technologies such as multiple-input–multiple-output (MIMO) antennas, beam-steering antennas, lens antennas, reconfigurable antennas, and metasurface-based antennas. In addition, antennas

✉ Uri Nissanov
uri1636@gmail.com

[1] Department of Electrical and Electronic Engineering Science, Auckland Park Kingsway Campus, University of Johannesburg, Johannesburg 2006, South Africa

technologies will need to be integrated by utilizing antenna on-chip (AoC) and antenna in-package (AiP) technologies [6, 9]. However, before D-band cellular communication can be used for 6G backhauling next-generation cellular communication, the antenna's gain needs to compensate these losses because of the power limitation of solid-state power sources resulting in very short communication distance propagation. Another possible solution to mitigate the high propagation losses of the atmosphere at THz band/D-band can be ultra-massive MIMO (UM-MIMO), beamforming, and beam-steering antennas [9]. Furthermore, the advantages of the UM-MIMO antennas can be expanded by enhancing the system gain diversity using an efficacious diversity antenna or transmitting numerous corresponding streams data to enhance data rates and spectral efficiency.

A beam-steering antenna is an electronically scanned phased array antenna controlled by a computer through phase shifters [10, 11]. Two sections can split up phase shifters. Analog phase shifters supply a tuneable continuous phase through a maximum and minimum phase shift angle using the Rotman lens [12] or Butler matrix [13]. However, digital phase shifters require different control voltages to straighten the control circuit, which causes less precise beam-steering, pendent on the number of phase bits [14]. Under the components that exist in contemporary technology, the central problem of the phase shifter at the D-band is the limited phase angle range up to about 0–30° [15]. However, the primary concern of D-band microstrip antenna fabrication is that the PCB technology requirements for a microstrip antenna are very tight, and the minimal fabrication etching can be around 0.05 mm. In comparison, the declared etching precision is about ± 0.01 mm [16]. Y. Zhang et al. [17] designed and simulated a W-band beam-steering ridge gap waveguide (RGW) array antenna at a resonance frequency of 95 GHz with the Ansys HFSS simulator. The beam-steering angle simulation results and the impedance BW were ± 40°, 20 GHz (21%). P. Lu et al. [18] designed and simulated THz beam-steering bow-tie antenna (BTA) with an integrated optical beam forming network (OBFN) chip at an operating frequency of 275–340 GHz with the Ansys HFSS simulator. The maximum directivity and steering angles obtained were 16 dBi, – 47° up to 25°, respectively. M. M. Islam et al. [19] designed and simulated an E-band beam-steering phased array 4 × 4 pyramidal horn antenna with meandered microstrip line used as a phase shifter on printed circuit board (PCB) at an operating frequency 71–86 GHz via the CST MWS simulator. The antenna was fabricated for experimental verification. The maximum measured gain, efficiency, and maximum steering angles obtained were 16.9 dB, – 3.2 dB, and 40°, respectively. M. Elkhouly et al. [20] designed and simulated a D-band transceiver forming a radio-on-glass (RoG) phased array front ends, which included an 8 × 16 slot antenna at operating frequency 142–156 GHz. The phased array included digital phase shifters. The transceiver was fabricated using a 0.13 µm SiGe BiCMOS process. The maximum gain, impedance BW, and beam-steering angles were 22 dB, 14 GHz, and – 16° up to 16°, respectively. M. Mantash et al. [21] designed and simulated a mmWave beam-steering leaky-wave antenna (LWA) hexagonal patch and a hexagonal loop and working frequency of 24–30 GHz. The impedance BW, gain, and steering angles simulation results with the CST MWS simulator were 6 GHz, 10.7 dB, and – 60° up to 60°. The antenna was fabricated for experimental verification. E. H. Mujammami et al. [22] designed and simulated a high-gain mmWave quasi-Yagi antenna array with Rotman lens beamforming network (BFN) at working frequency 24–40 GHz. The impedance BW, gain, and steering angles simulation results with the CST MWS simulator were 16 GHz, 14 dB, and –40° up to 40°. The antenna was fabricated for experimental verification.

From the reported literature, it may have been shown that there is still no D-band Rotman lens beam-steering microstrip array antenna, with a phase-shifting angle of more than 30°, which can be used for 6G cellular communication antennas at 110–145 GHz.

This paper explores a design flowchart, design equations, and design and simulation of a D-band Rotman lens beam-steering microstrip array antenna at 110–145 GHz operating frequency. The design and simulation were with the time-domain solver at the CST MWS simulator, while the comparison was with the frequency-domain solver at the CST MWS simulator.

The paper's innovation was to design a D-band Rotman lens beam-steering microstrip array antenna with novel 1 × 8 radiators for 6G backhauling cellular communication at an operating frequency of 110–145 GHz. The proposed method can suggest designing and future fabricating a D-band beam-steering microstrip array antenna with a phase-shifting angle of more than 30°, which is the primary concern at the D-band beam-steering for 6G backhauling cellular communication antennas. Furthermore, to reduce the extremely high cost of experimental validation with prototype fabricated, D-band Rotman lens beam-steering microstrip array antenna, the design was compared with another solver at the CST MWS simulator.

2 Proposed antenna design and analysis

The design included a couple of stages. The first is the design and simulation of the D-band Rotman lens with the Remcom Rotman lens designer (RLD) software. For more precise simulation, we use a full-wave 3D CST MWS simulator. The second stage is designing and optimizing a D-band single radiator on a microstrip laminate with the CST MWS simulators. Next,

on a base of the optimized radiator, design and simulate a D-band 1×8 microstrip array antenna, incorporate the D-band Rotman lens with D-band 1×8 microstrip array antenna, and optimize the D-band Rotman beam-steering microstrip array antenna.

2.1 Principle operation and equations for the Rotman lens

Highly directional transmission is necessary to mitigate the high atmospheric absorption and path loss at D-band. Thus, tunable antenna arrays with efficacious BFN and fair beam-steering abilities are used to merge signals of radiators into a pattern, which is further directive than the individual radiator pattern. A BFN is generally composed of output and input ports organized along an arc. All input port at the focal layer supplies the desired phase and amplitude distribution so that the antenna beam is directed at a particular angle [22, 23]. Rotman lenses are BFN and sustain low phase error, broadband, and broad-angle beam-steering. In addition, they are the true-time-delay (TTD) apparatus supplying non-dependent frequency beam-steering. The RLD software is founded on Geometrical Optics with the Rotman lens equations [24, 25] and analyzes the Rotman lens with a rapid design tool. The analysis with the RLD software is based on the following assumptions: transmission line, material dispersion, and parasitic coupling are of a lesser degree. Radiative leaks are not accounted for, and the dummy load is ideal without losses. Figure 1 shows the Rotman lens configuration.

The transmission line lengths and lens inner contour points are solved for using the path length comparison method as in [24, 25]:

$$\overrightarrow{F_1P} + W + N\sin\alpha = F + W_0 \tag{1}$$

$$\overrightarrow{F_2P} + W - N\sin\alpha = F + W_0 \tag{2}$$

$$\overrightarrow{F_0P} + W = G + W_0 \tag{3}$$

where

$$\left(\overrightarrow{F_1P}\right)^2 = (F\cos\alpha + X)^2 + (F\sin\alpha - Y)^2 \tag{4}$$

$$\left(\overrightarrow{F_2P}\right)^2 = (F\cos\alpha + X)^2 + (F\sin\alpha + Y)^2 \tag{5}$$

$$\left(\overrightarrow{F_0P}\right)^2 = (G + X)^2 + (Y)^2 \tag{6}$$

Lens dimensions are then normalized by the off-axis focal length [24]:

$$\eta = N/F \tag{7}$$

$$g = G/F \tag{8}$$

$$x = X/F \tag{9}$$

$$y = Y/F \tag{10}$$

$$w = \frac{W - W_0}{F} \tag{11}$$

For x, y, w, we can get:

$$y = \eta(1 - w) \tag{12}$$

$$x^2 + y^2 + 2a_0x = w^2 + b_0^2\eta^2 - 2w \tag{13}$$

$$aw^2 + bw + c = 0 \tag{14}$$

where

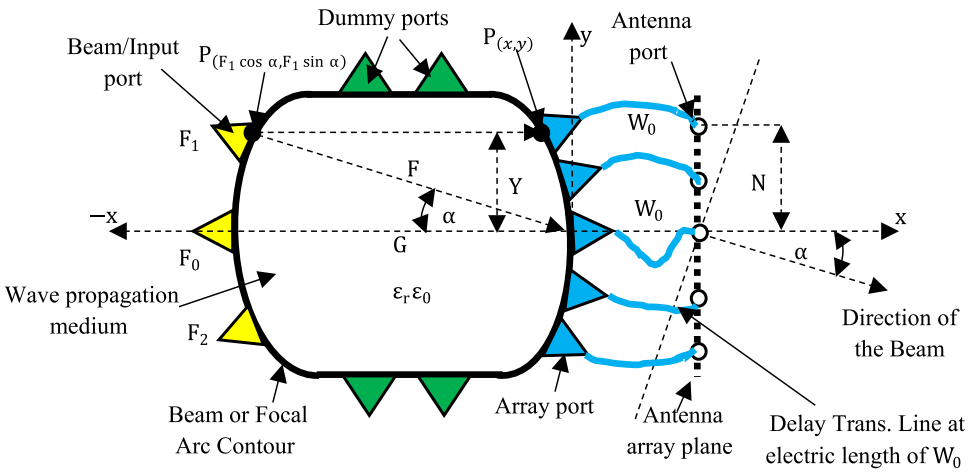

Fig. 1 Rotman lens configuration

$$a = 1 - \eta^2 - \left(\frac{g-1}{g-a_0}\right) \tag{15}$$

$$b = \left[2g\left(\frac{g-1}{g-a_0}\right) - \left(\frac{g-1}{(g-a_0)^2}\right)b_0^2\eta^2 + 2\eta^2\right] - 2g \tag{16}$$

$$c = \frac{gb_0^2\eta^2}{g-a_0} - \frac{b_0^4\eta^4}{4(g-a_0)^2} - \eta^2 \tag{17}$$

where η is the element gapping—the gapping of the radiators along with the outer profile, g is the focal ratio—the ratio of on-axis focal distance to off-axis focal distance, lens width (G or F_0) is the length between the middle of the focal profile and the middle of the array profile, and scan angle (α) is the direction of the main beam, which phase error is null. The RLD software solves these points each time F, η, α, g are modified.

When the lens profile is well thought out, the transmission line electrical length for standard microstrip design equations is used to find the line width of the transmission lines [26]:

$$\frac{W}{d} = \left\{ \begin{array}{l} \frac{8e^A}{e^{2A}-2} \rightarrow \text{ for } \frac{W}{d} < 2 \\ \frac{2}{\pi}\left[B - 1 - \ln(2B-1) + \frac{\varepsilon_r - 1}{2\varepsilon_r}\left\{\ln(B-1) + 0.39 - \frac{0.61}{\varepsilon_r}\right\}\right] \rightarrow \text{ for } \frac{W}{d} > 2 \end{array} \right\} \tag{18}$$

where

$$A = \frac{Z_0}{60}\sqrt{\frac{\varepsilon_r - 1}{\varepsilon_r + 1}} + \frac{\varepsilon_r - 1}{\varepsilon_r + 1}\left(0.23 + \frac{0.11}{\varepsilon_r}\right) \tag{19}$$

$$B = \frac{377\pi}{Z_0\sqrt{\varepsilon_r}} \tag{20}$$

The ratio, which is used to calculate the effective dielectric constant (ε_{eff}), is:

$$\varepsilon_{eff} = \left(\frac{\varepsilon_r + 1}{2}\right) + \left(\frac{\varepsilon_r - 1}{2}\right)\frac{1}{\sqrt{1 + 12d/W}} \tag{21}$$

The transmission lines port impedance can be calculated by using:

$$Z = \left\{ \begin{array}{l} \frac{60}{\sqrt{\varepsilon_{eff}}}\ln\left(\frac{8d}{W} + \frac{W}{4d}\right) \rightarrow for\frac{W}{d} \le 1 \\ \frac{120\pi}{\sqrt{\varepsilon_{eff}}\left[\frac{W}{d} + 1.393 + 0.667\ln\left(\frac{W}{d} + 1.444\right)\right]} \rightarrow for\frac{W}{d} \ge 1 \end{array} \right\} \tag{22}$$

2.2 The design procedure flowchart of the Rotman lens beam-steering microstrip array antenna

The design procedure of the Rotman lens beam-steering microstrip array is presented in Fig. 2. Typically, the design procedure starts with the design of the Rotman lens with the RLD software. We need to define the frequency of operation, array dimensions, scan angle, the number of beams, electrical characteristics of the lens material, BW, physical size, and shape limitations. The RLD will use these parameters and calculate the dimensions of the Rotman lens with minimal phase errors. Any changes with the above parameters will change the dimensions of the Rotman lens. Next, the designer can plot the 2D simulation results with the Geometrical Optics combined with the classical Rotman lens equations [24, 25], such as the array factor, beam to phase error, array to beam coupling magnitude. If the results are good enough, the lens geometry can be exported by computer-aided design (CAD) to a 3D full-wave analysis simulator. If the 3D full-wave analysis of the Rotman lens is good enough, we can combine the proposed design with a suitable radiators array design and simulate it with 3D full-wave simulator, and else we need to redesign the Rotman lens with the RLD software.

The proposed flowchart may be used to design different antennas after appropriate modification.

2.3 The suggested D-band Rotman lens

The D-band Rotman lens was made with Isola Astra MT77 microstrip laminate with the copper thickness (t), substrate height (h), ε_r, and tanδ of 17.5 µm, 127 µm, 2.82, 0.001@125 GHz, respectively; Fig. 3 shows the suggested D-band Rotman lens. Every dummy port is terminating with a discrete port condition with an impedance of 50 ohms.

The parameters of the Rotman lens, which was inserted into RLD software, are present in Table 1.

2.4 The suggested D-band Rotman lens beam-steering microstrip array antenna

The D-band Rotman lens beam-steering microstrip array antenna is based on the same laminate and parameters as the Rotman lens laminate. Figure 4 shows the suggested D-band Rotman lens beam-steering microstrip array antenna. The

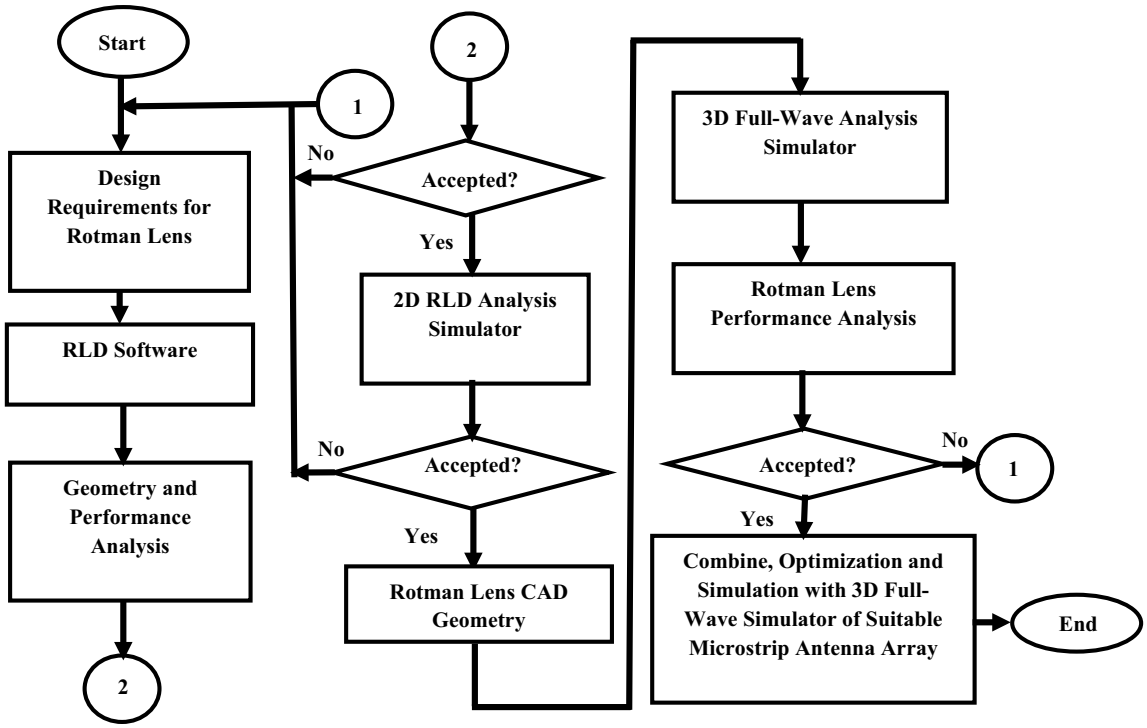

Fig. 2 Design procedure flowchart of the Rotman lens beam-steering microstrip array antenna

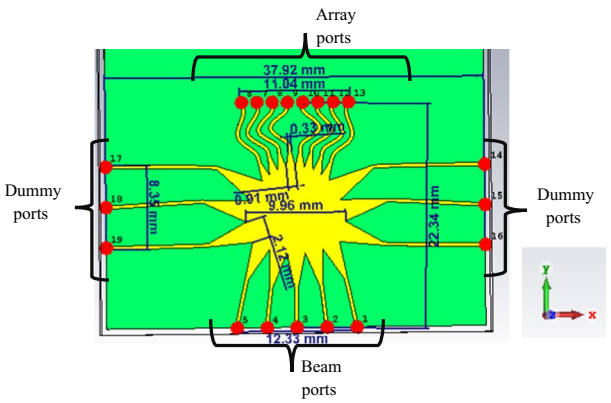

Fig. 3 Suggested D-band Rotman lens

dimensions of the substrate were $37.92 \times 30 \times 0.127$ mm^3 that equals $15.8\lambda_0 \times 12.5\lambda_0 \times 0.53\lambda_0$@125GHz, where λ_0 is the free-space wavelength.

Table 1 Design parameters defined into RLD software

Parameter	Value at RLD 1.7
Copper conductor thickness (t)	17.5 µm
Substrate thickness (h)	127 µm
Substrate permittivity (ε_r)	2.82 @ 125 GHz
Substrate loss tangent (tanδ)	0.001@125 GHz
Length x width x height	$37.92 \times 22.34 \times 0.127$ mm^3
Center frequency	125 GHz
Bandwidth	±20 GHz → 125 GHz ± 20 GHz
Beamwidth	30°
Max. scan angle	±30°
Focal angle (Flare angle)	12°
Array number output ports	8
Number of beams	5
Dummy ports	6
Z system	50 ohms
Port width	334 µm

3 Simulation, comparison of results and discussion

The best way to validate the design of the simulated proposed beam-steering antenna is by experimental verification, but if we want to reduce the high cost, we can use

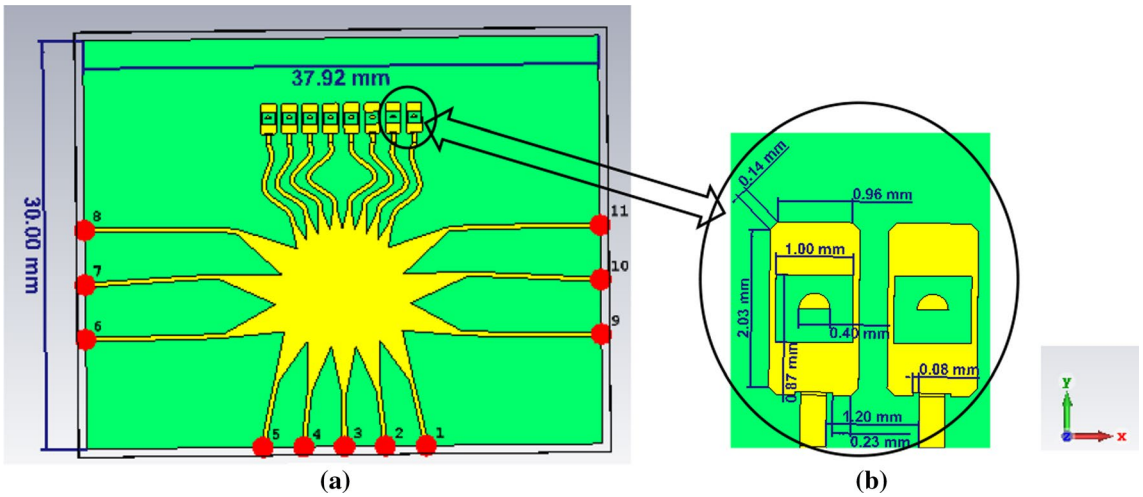

Fig. 4 Suggested D-band Rotman lens beam-steering microstrip array antenna, **a** front size of the suggested antenna, **b** zoom partial size of radiators and their dimensions

simulator comparisons with different solver techniques [16], and if we want that the comparison will be close as much as can be to experimental verification, we must define at both solver the ε_r and tanδ of the antenna laminate, which are frequencies dependent, as close to our working frequencies (110–145 GHz), so the simulation with two different solvers has been chosen at the proposed beam-steering microstrip array antenna.

The initial design of the Rotman lens was done with Remcom RLD software. In comparison, the modeling and the simulation of the suggested D-band Rotman lens beam-steering microstrip array antenna were with the 3D full-wave time-domain solver based on finite integration technique (FIT) at CST MWS simulator version 2020. The comparison of the suggested antenna was with the frequency-domain solver based on finite element modeling (FEM) at CST MWS simulator version 2020.

3.1 The suggested D-band Rotman lens simulation results

Figure 5 illustrates the S-parameter $\left(S_{11} - S_{13,1} \right)$ simulation results of suggested D-band Rotman lens. It has been shown that the BW$\left(\left[S_{11} \& S_{21} \& S_{31} \& S_{41} \& S_{51} \right] \leq -15\text{dB} \right)$ of the D-band Rotman lens is: > 50 GHz$(> 40\%)$ while the resonances frequencies are between 100 and 150 GHz and the insertion losses $\left(S_{61} \& S_{71} \& S_{81} \& S_{91} \& S_{10,1} \& S_{11,1} \& S_{12,1} \& S_{13,1} \right)$ are between –10.28 and –19.93 dB.

Figure 6a–b illustrates the S-parameter phases $\left(\sphericalangle S_{6,1} - \sphericalangle S_{13,1} \right)$ in [°] vs. frequency at GHz of the suggested D-band Rotman lens. Figure 6a shows that the S-parameter phases $\left(\sphericalangle S_{6,1} - \sphericalangle S_{13,1} \right)$ are between –180° and 180°. Furthermore, Fig. 6b shows that the average changes of the S-parameter phases $\left(\sphericalangle S_{6,1} - \sphericalangle S_{13,1} \right)$ between the

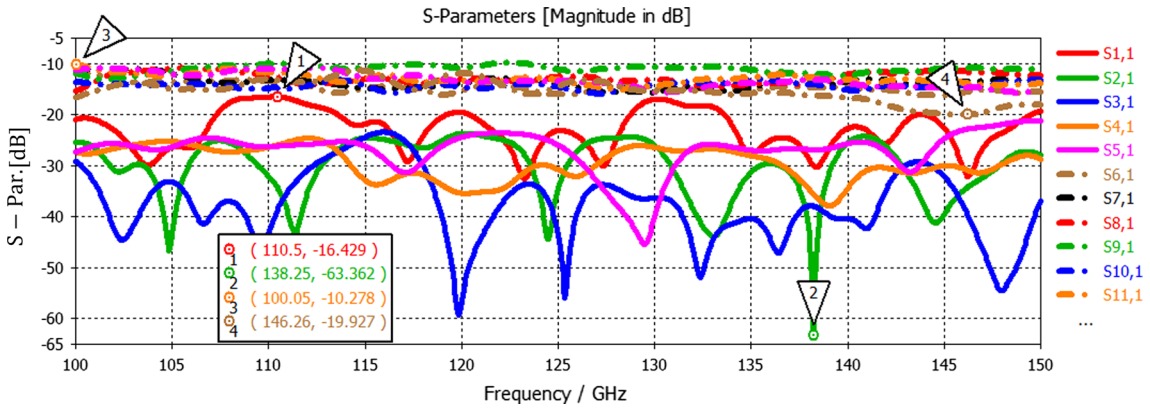

Fig. 5 Simulation results of S-parameters $\left(S_{11} - S_{13,1} \right)$ of the suggested D-band Rotman lens

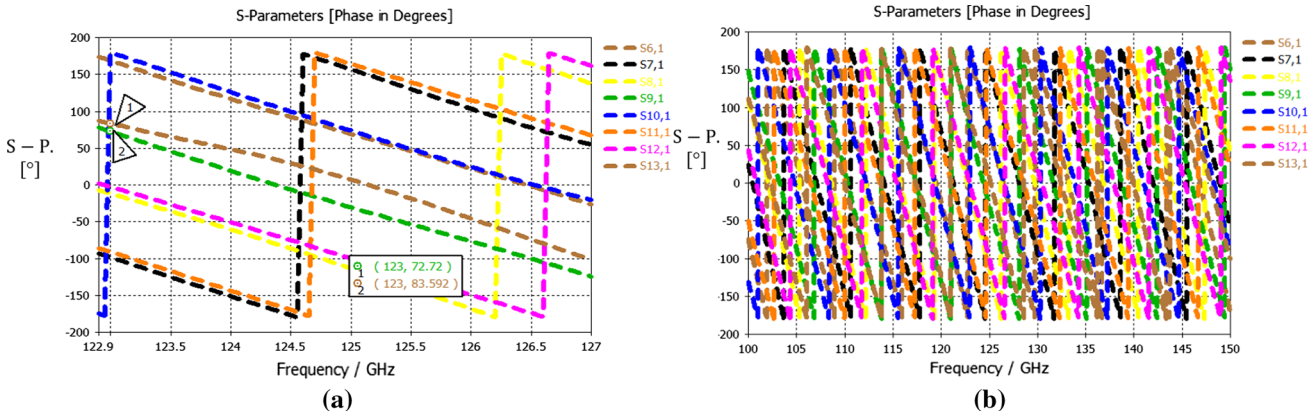

Fig. 6 **a**–**b**: Simulation results of the S-parameter phases $\left(\sphericalangle S_{6,1} - \sphericalangle S_{13,1}\right)$ of the suggested D-band Rotman lens

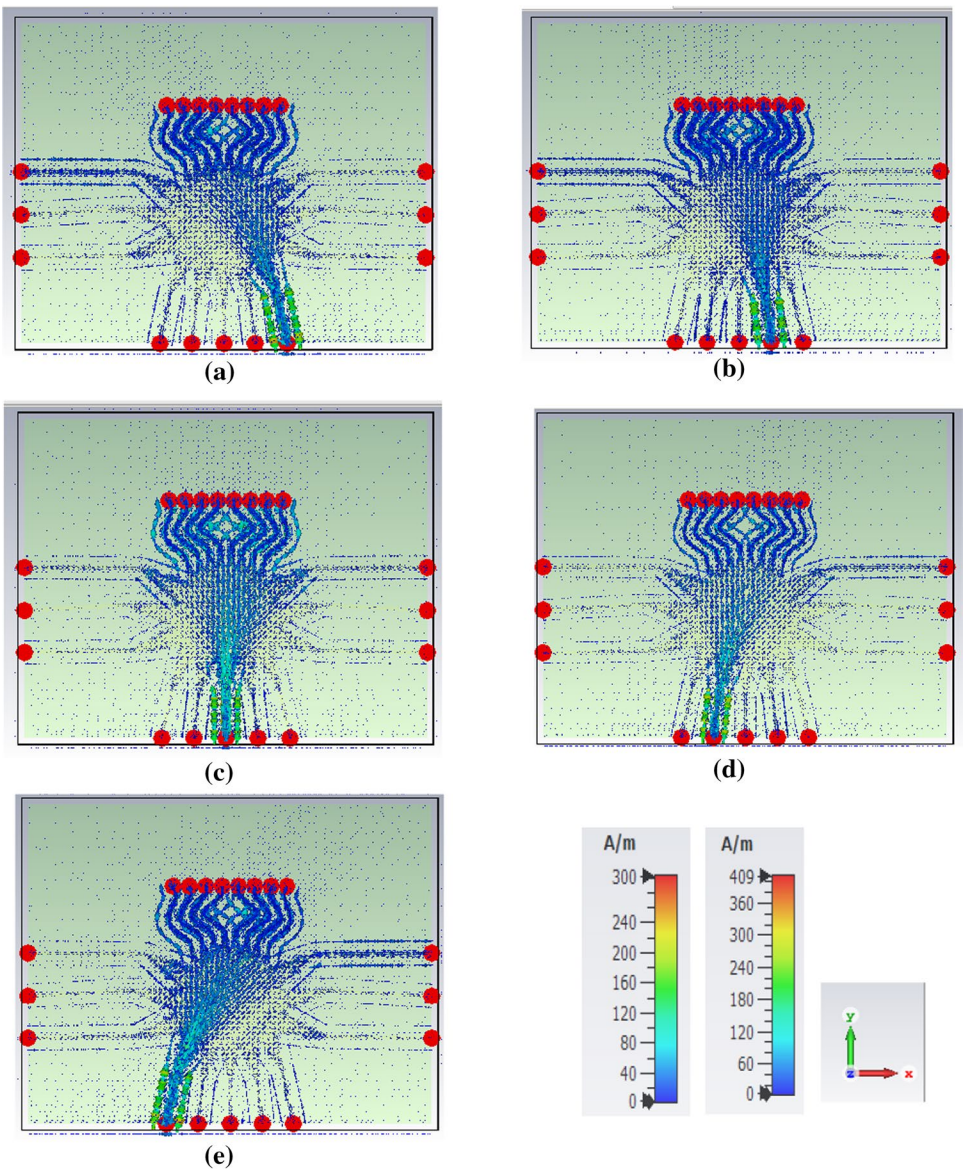

Fig. 7 **a**–**e**: Surface current of the proposed optimized D-band Rotman lens with **a** Port 1 excited, **b** Port 2 excited, **c** Port 3 excited, **d** Port 4 excited, **e** Port 5 excited

array port and subsequent array port of the suggested D-band Rotman lens is 11.1°.

Figure 7a–e illustrates the surface current of the suggested D-band Rotman lens when each Port 1 up to Port 5 is excited separately. Figure 7a–e shows that the surface current of the suggested D-band Rotman lens is between 300 and 409 A/m.

3.2 The simulation results of the suggested D-band Rotman lens beam-steering microstrip array antenna

Figure 8a–c illustrates the simulation result of return losses $(S_{11}, S_{22}, S_{33}, S_{44}, S_{55})$, realized gain, and the suggested D-band Rotman lens beam-steering microstrip array antenna's total efficiency. Figure 8a shows that the

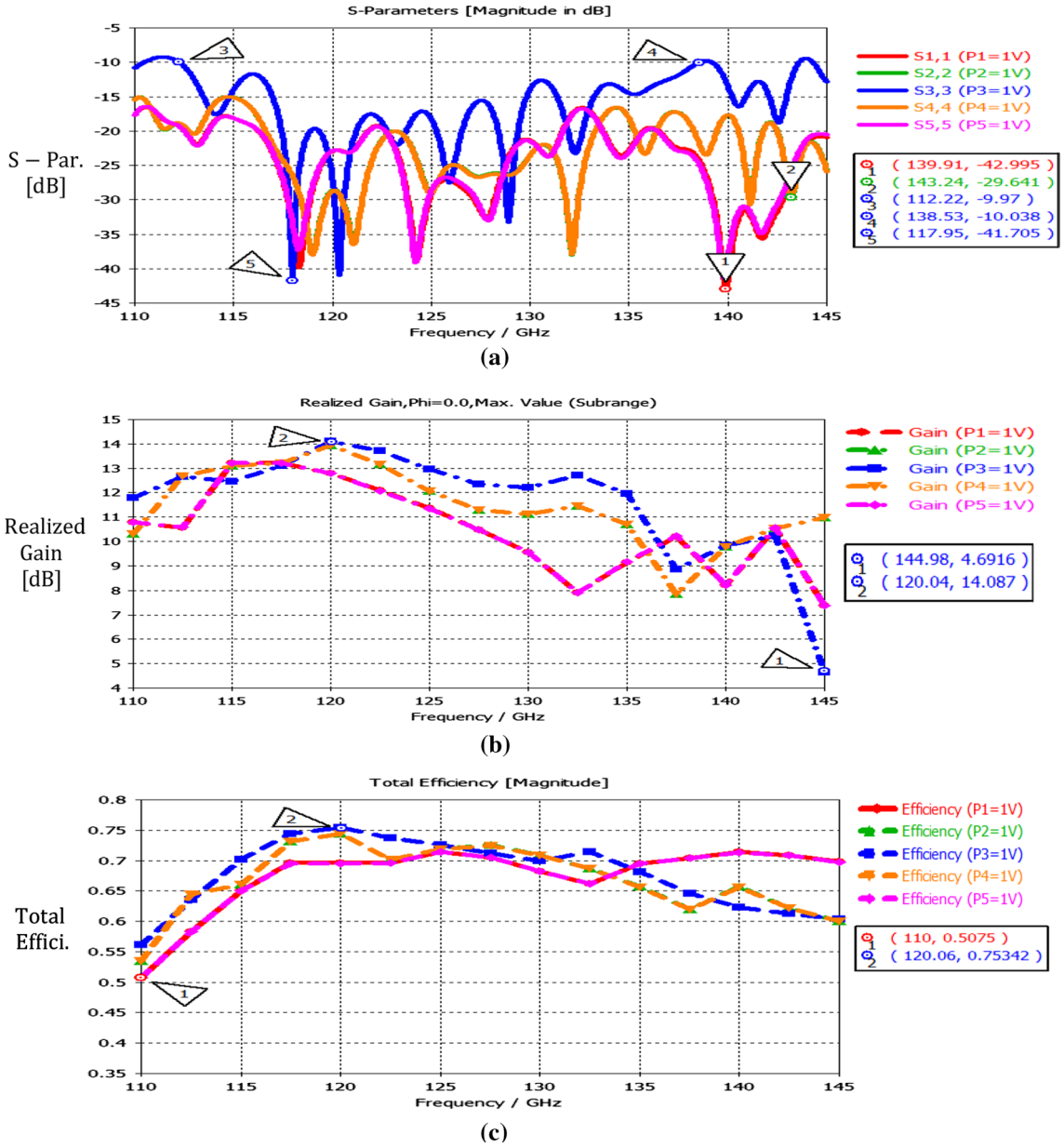

Fig. 8 Simulation result for the suggested D-band Rotman lens beam-steering microstrip array antenna: **a** return loss, **b** gain, **c** total efficiency

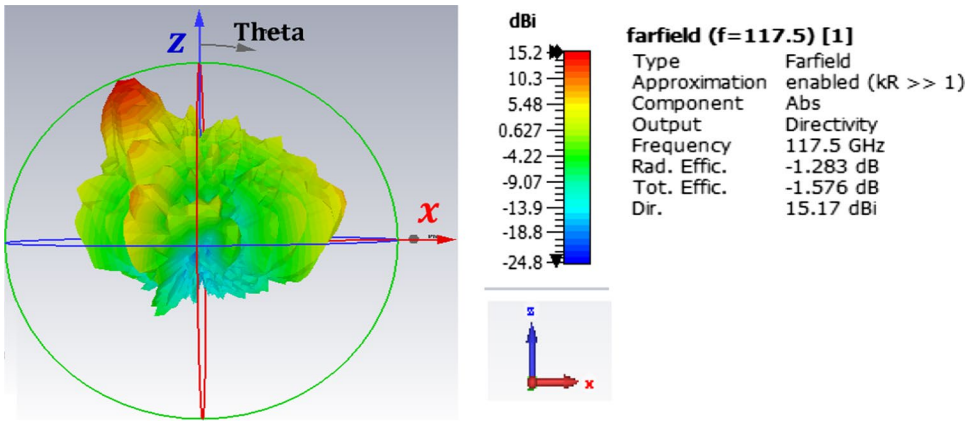

Fig. 9 Simulation result of the directivity radiation pattern of the suggested D-band Rotman lens beam-steering microstrip array antenna for 117.5 GHz

$\mathrm{BW}(S_{11}, S_{22}, S_{33}, S_{44}, S_{55} \leq -10\,\mathrm{dB})$ of the antenna is 31.02 GHz(24.3%) while the resonance frequencies are between 117.95–143.24 GHz. Figure 8b shows that the realized gain of the antenna is between 4.69 and 14.09 dB. Figure 8c shows that the total efficiency of the antenna is between 50.75 and 75.34% at 110–145 GHz.

Figure 9 illustrates the simulation result of the directivity radiation pattern of the suggested D-band Rotman lens beam-steering microstrip array antenna for 117.5 GHz. Figure 9 shows that the directivity, radiation efficiency, and total efficiency of the suggested D-band Rotman lens beam-steering microstrip array antenna for 117.5 GHz is 15.2 dBi, – 1.28 dB, and – 1.57 dB, respectively.

Figure 10a–f illustrates the simulation results of the E-field of the suggested D-band Rotman lens beam-steering microstrip array antenna depending on the frequencies of 115 GHz, 125 GHz, and 135 GHz and to the beam-steering angles when each Port 1 up to 5 is excited separately. Figure 10a–f shows that the E-field levels of the antenna are between 9.6 and 13.92 dB. At the same time, the beam-steering angles are between –23.35° and 23.76°.

3.3 Comparison of simulation results of the suggested D-band Rotman lens beam-steering microstrip array antenna with declared etching accuracy

The antenna, a resonance component, dimensions depend on the wavelength. At higher frequencies, the wavelength is smaller, so the antenna dimensions are also smaller; so, when we fabricated the proposed D-band Rotman lens beam-steering microstrip array antenna, the minimal PCB fabrication etching can be around 0.05 mm, while the declared PCB etching precision is about ± 0.01 mm [16]. Thus, the minimal PCB etching at the proposed beam-steering antenna design dimensions was not below 0.05 mm.

Simulations were also executed on the possibility of declared etching precision, i.e., for each eight radiator's sizes to illustrate the possible errors of future proposed prototype D-band Rotman lens beam-steering microstrip array antenna fabrication for experimental verification. The possible fabrication declared PCB etching precision was subtracted/added in the CST MWS simulator, and two more simulations were performed with the new values. Therefore, three more graphs were attained for the realized gain, S_{11}, and beam-steering angle when Port 1 is excited, which may show the realized gain, S_{11}, and beam-steering angle, which can be attained in the prototype fabricated D-band Rotman lens beam-steering microstrip array antenna.

Figure 11a–c illustrates the comparison of the simulation results of the S_{11}, the realized gain and E-field for 110 GHz and 135 GHz of the suggested D-band Rotman lens beam-steering microstrip array antenna, which Port 1 excited with or without future fabrication declared PCB etching precision ± 0.01 mm [16]. Figure 11a shows that the $\mathrm{BW}_{S_{11<-15\,\mathrm{dB}}}$ of the future fabricated D-band Rotman lens beam-steering microstrip array antenna will not be changed and will be 31.02 GHz due to declared PCB etching precision. The same as the simulated proposed D-band Rotman lens beam-steering microstrip array antenna. From Fig. 11b, the realized gain of the future fabricated D-band Rotman lens beam-steering microstrip array antenna may have been shown by 0.1 dB from the simulated proposed D-band Rotman lens beam-steering microstrip array antenna due to declared PCB etching precision. Figure 11c shows the beam-steering angle will change by 1 degree from the simulated proposed D-band Rotman lens beam-steering microstrip array antenna due to declared PCB etching precision.

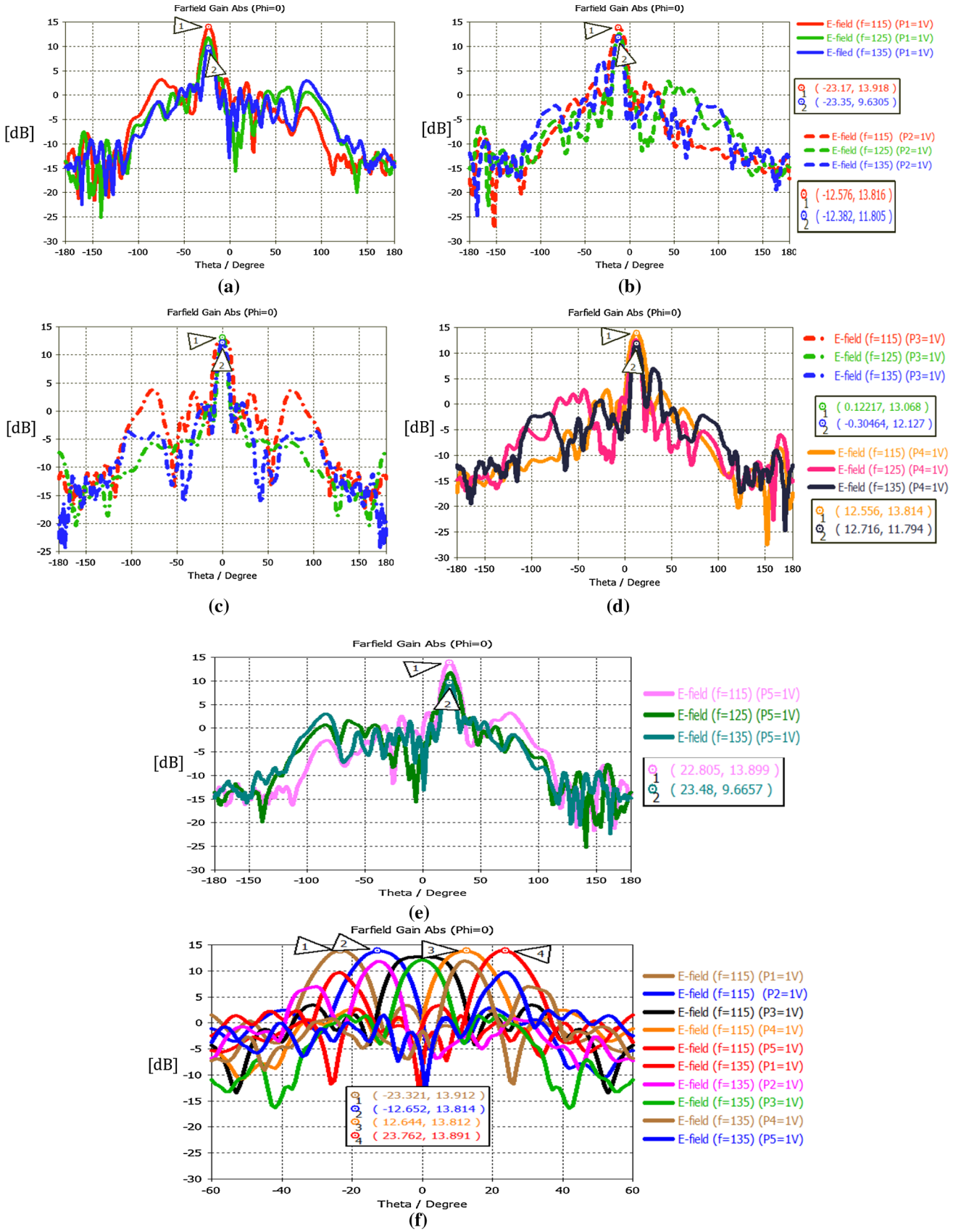

Fig. 10 Simulation results of the E-field for the suggested D-band Rotman lens beam-steering microstrip antenna with **a** Port 1 excited, **b** Port 2 excited, **c** Port 3 excited, **d** Port 4 excited, **e** Port 5 excited, **f** Combining all simulation results

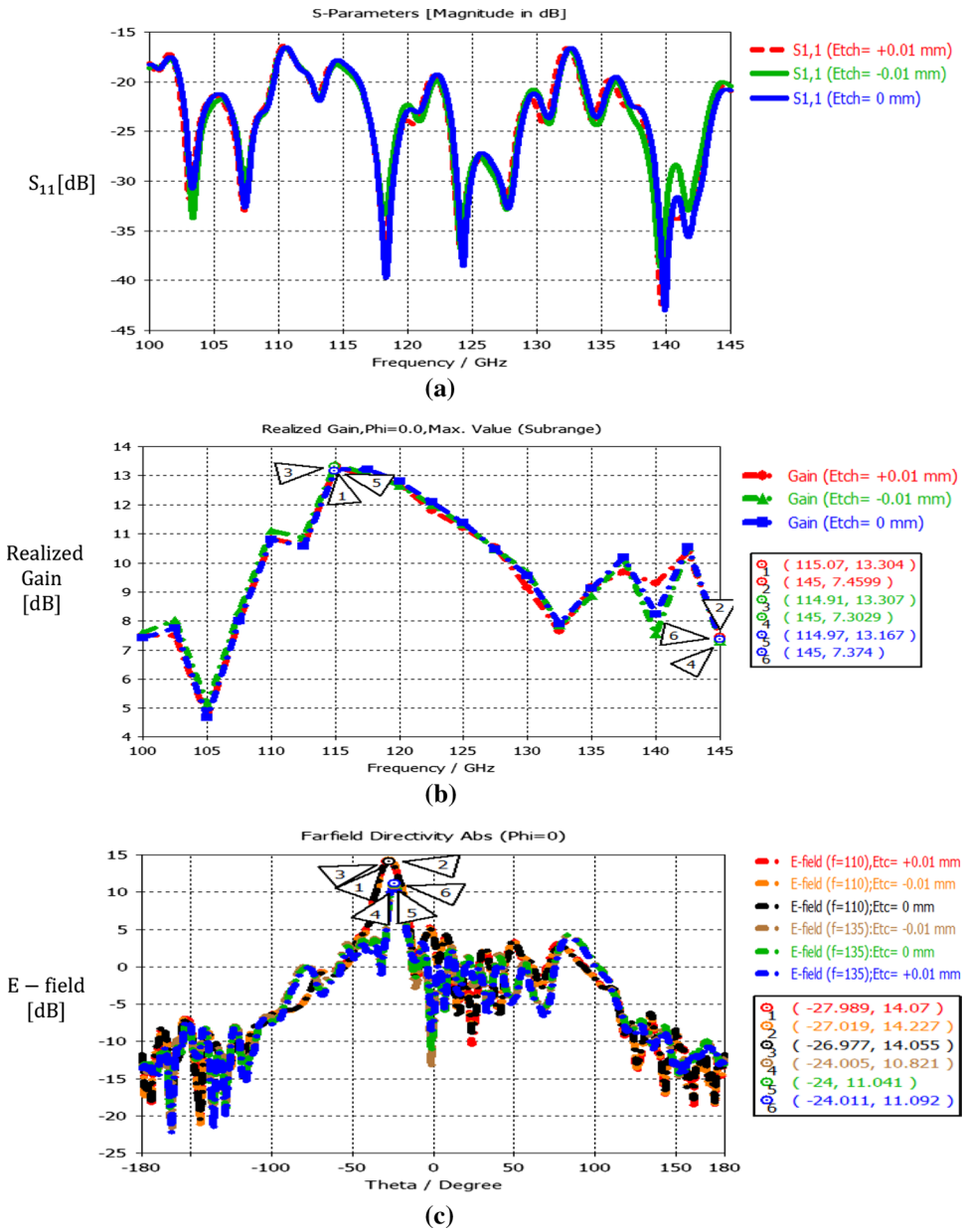

Fig. 11 Simulation results in comparison of the suggested D-band Rotman lens beam-steering microstrip array antenna with the declared etching precision, **a** S_{11}, **b** realized gain, **c** E-field for 110 GHz and 135 GHz

3.4 Comparison of the simulation results of the suggested D-band Rotman lens beam-steering microstrip array antenna

Figure 12a–b illustrates the comparison of the simulation results of the return loss and the realized gain of the suggested D-band Rotman lens beam-steering microstrip array antenna, which Port 1 excited and done with FIT CST MWS and FEM CST MWS simulator. Figure 12a shows that the BW of the suggested D-band Rotman lens beam-steering microstrip array antenna is the same at both of the solvers. Figure 12b shows that the realized gain of the suggested D-band Rotman lens beam-steering microstrip antenna from the FEM CST MWS simulator is between 7.46 and 14.16 dB, and the realized gain of the antenna from the FIT CST MWS simulator is between 4.67 and 13.2 dB. So Fig. 12a–b shows that a good agreement between the simulation results is achieved concerning the suggested D-band Rotman lens beam-steering microstrip antenna, which validates the proposed design flowchart design, design equations, and designed D-band Rotman lens beam-steering microstrip array antenna.

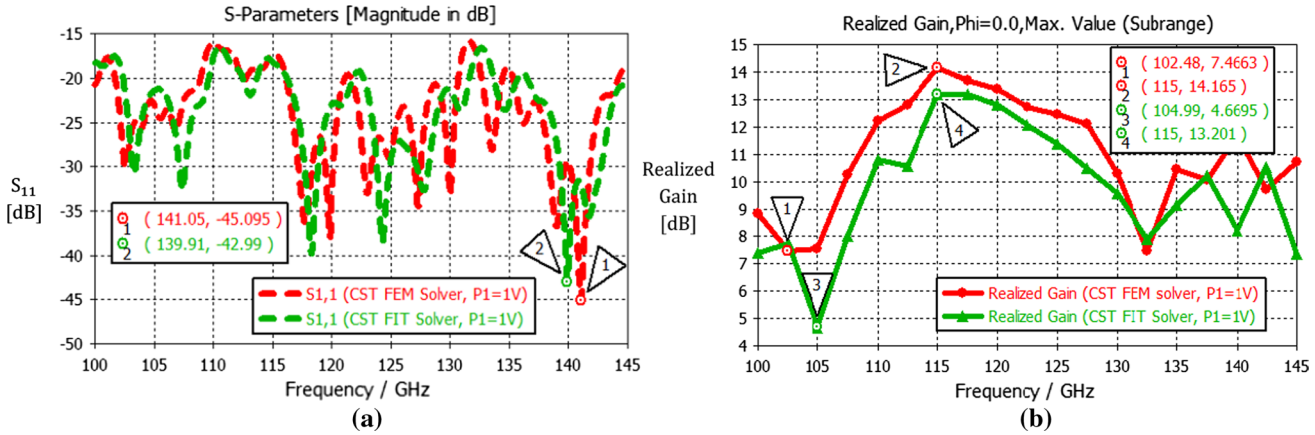

Fig. 12 Comparison of the simulation results of the suggested D-band Rotman lens beam-steering microstrip array antenna made with FIT CST MWS and FEM CST MWS simulator, **a** the S_{11}, **b** the realized gain

3.5 Discussion

Highly directional antennas with efficacious BFN and fair beam-steering abilities are used to merge signals of radiators into a pattern to mitigate the high atmospheric absorption and path loss at D-band for backhauling next-generation cellular communication at the 6G [22, 23].

The purpose of this paper was to present a design flowchart, design equations, and to design and simulate a D-band Rotman lens beam-steering microstrip array antennas at an operating frequency of 110−145 GHz for 6G backhauling cellular communication with the FIT solver at CST MWS simulator, while the comparison of the simulations results of the offered antenna was with FEM solver at CST MWS simulator. Following the simulation result with the FIT solver at the CST MWS simulator, the $\mathrm{BW}\left(\left[S_{11}\&S_{21}\&S_{31}\&S_{41}\&S_{51}\right] \le -15\mathrm{dB}\right)$ of the D-band Rotman lens was > 50 GHz(> 40%). The peak realized gain, peak BW, peak total efficiency, and peak steering angles obtained for the proposed D-band Rotman lens beam-steering microstrip array antenna were 14.09 dB, > 35 GHz, 75.34%, and (–23.35°) up to 23.76°, respectively. The proposed simulation results of the D-band Rotman lens beam-steering microstrip array antenna for Port 1 excited were compared with the FEM solver at the CST MWS simulator. The peak realized gain and BW were 14.16 dB and > 35 GHz, while from the FIT solver at CST MWS simulator, the peak realized gain and BW were 13.2 dB and > 35 GHz, so a good agreement was achieved, which validated the proposed design flowchart, design equations, and the proposed D-band Rotman lens beam-steering microstrip array antenna.

This paper presents that the proposed work's simulation results were compared with different solver techniques comparison [16]. The comparison was to reduce the high cost of experimental verification and to show the possible errors on the realized gain, BW/S_{11} and beam-steering angle, due to PCB machinery etching precision ± 0.01 mm [16] when the proposed antenna will be prototype fabricated for experimental verification, where two new simulations were performed with the PCB machinery etching precision. From these new simulation results, the realized gain, BW/S_{11} and beam-steering angle will not change dramatically when the proposed D-band Rotman lens beam-steering microstrip array antenna is fabricated due to PCB etching precision, and in order that the comparison will be close as much as can be we defined at both solver the ε_r and tanδ of the antenna laminate, which are frequencies dependent, which were defined at a frequency of 125 GHz, reasonably close to our working frequencies 110–145 GHz. In works [19–22], the simulation results were validated by the fabrication and measurement of a prototype beam-steering antenna. The beam-steering technology in the proposed paper was by Rotman lens, an analog beam-steering the same as [19, 21, 22], while in [18, 20], the beam-steering were OFBN and digital beam-steering, respectively. This beam-steering antenna was designed for D-band the same as [20]. In [17, 19, 21, 22], the beam-steering antenna was designed for mmWave up to 95 GHz, and [18] was for 300 GHz. The proposed beam-steering antenna was achieved the highest BW up to 170 GHz compared to [17, 19, 21, 22]. As work [20] was fabricated for experimental verification and needed a D-band digital phase shifter, the proposed design can be fabricated without needing a D-band phase shifter where under the components that exist in contemporary technology, the central problem of the phase shifter at the D-band is the limited phase angle range up to about 0–30° [15]. With the proposed method, we can design and fabricate a D-band beam-steering microstrip array antenna with a phase-shifting angle of more than 30° and more significant gain by a more

Table 2 Comparison with others reported kinds of literature

Refs.	Antenna tech	Beam-steering tech	Nomi. freq. (GHz)	Peak directivity/gain (dBi/dB)	BW (GHz)	Beam-steering angle range (°)	Valid
[17]	W-band RGW array	n/a	95	n/a	20	±40	n/a
[18]	Bow tie	OBFN	300	16 dBi	65	− 47 up to 25	n/a
[19]	E-band phased array 4×4 pyramidal horn	Analog microstrip delay lines	78.5	16.9 dB	15	40	Exp
[20]	D-band 8×16 slot	Digital	149	22 dB	14	±16	Exp
[21]	mmWave LWA	Analog LWA	27	10.7 dB	6	±60	Exp
[22]	mmWave Quasi-Yagi	Analog Rotman lens	32	14 dB	16	±40	Exp
This work	D-band microstrip 1×8 array	Analog Rotman lens	118–143	Realized gain—14.09 dB	>35	±23.8	Solver comp

extensive array. However, the primary concern of D-band microstrip antenna fabrication is that the PCB technology requirements for a microstrip antenna are very tight [16] and described above. Table 2 is attached to show the comparison with reported pieces of literature.

4 Conclusions

This paper presents a design flowchart, design equations, and design of a D-band Rotman lens beam-steering microstrip array antenna. First, the initial design of the Rotman lens was done by Remcom RLD software. Then, the Rotman lens geometry was exported to a 3D full-wave analysis with the FIT solver at the CST MWS simulator and embedded with state-of-the-art microstrip radiators. As a result, the peak realized gain, peak BW, peak total efficiency, and peak steering angles obtained for the proposed D-band Rotman lens beam-steering microstrip array antenna were 14.09 dB, >35 GHz, 75.34%, and –23.35° up to 23.76°, respectively. With the proposed method, we can design and fabricate a D-band beam-steering microstrip array antenna with a phase-shifting angle of more than 30° and a more significant gain of more than 14.09 dB with a more extensive array. Furthermore, the simulation results of the beam-steering antenna were compared with the FEM solver at the CST MWS simulator, and the obtained simulatin results were close to each other, which validated the design flowchart and equations and the design of the proposed D-band Rotman lens beam-steering microstrip array antenna. Thus, the proposed D-band Rotman lens beam-steering microstrip array antenna can be a proper candidate for next-generation backhauling cellular communication at the 6G. However, an experimental verification with the fabrication of the proposed D-band Rotman lens beam-steering microstrip array antenna is needed for more precise validation.

Acknowledgements Thanks to REMCOM company Ltd, which lent for a limited time the Rotman lens designer (RLD) software by the Israeli distributor, Synergy Integration Ltd.

Funding No funding was received to assist with the preparation of this manuscript.

Availability of data and materials Upon request, the author will send the design and simulation results with the CST MWS simulator.

Declarations

Conflict of Interest The author has no conflicts of interest to declare relevant to the content of this article.

References

1. Vassilev, V., He, Z.S., Carpenter, S., Zirath, H., Yan, Y., Hassona, A., Bao, M., Emanuelsson, T., Chen, J., Horberg, M., Li, Y., Hansryd, J.: Spectrum efficient D-band communication link for real-time multi-gigabit wireless transmission. In: IEEE/MTT-S International Microwave Symposium (IMS), Philadelphia, PA, USA, 10–15 June 2018, pp. 1523–1526
2. Frecassetti, M.G.L., Mazzanti, A., Sevillanoiabal, J.F., del-Río, D., Ermolov, V.: D-band transport solution to 5G and beyond 5G cellular networks. In: IEEE European Conference on Networks and Communications (EuCNC), Valencia, Spain, 18–21 June 2019, pp. 1–5
3. Liu, M.: Research on the development of intelligent logistics based on 5G technology. In: IEEE 2nd International Conference on Urban Engineering and Management Science (ICUEMS), Sanya, China, 29–31 Jan. 2021, pp. 1–3
4. Oestges, C., Quitin, F.: Inclusive radio communications for 5G and beyond, 1st edn., pp. 1–394. Elsevier, Amsterdam (2021)
5. CISCO-Internet of Everything (IoE): Top 10 Insights from Cisco's IoE value at stake analysis for the public sector. https://www.cisco.com/web/about/ac79/docs/innov/IoE.pdf

6. Padhi, P.K., Charrua-Santos, F.: 6G enabled industrial internet of everything: towards a theoretical framework. MDPI Appl. Syst. Innov. **4**(1), 1–28 (2021)
7. Milovanovic, D., Bojkovic, Z.: 5G mobile networks: what is subsequent. Int. J. Commun. **4**, 1–5 (2019)
8. Jha, K.R., Singh, G.: Terahertz Planar Antennas for Next-Generation Communication. Springer, Berlin (2014)
9. Tekbiyik, K., Ekti, A.R., Kurt, G.K., Gorcin, A.: Terahertz band communication systems: challenges, novelties and standardization efforts. Phys. Commun. **35**(100700), 1–28 (2019)
10. Fu, X., Yang, F., Liu, C., Wu, X., Cui, T. J.: Terahertz beam steering technologies: from phased arrays to field-programmable metasurfaces. Adv. Opt. Mater., no. 1900628, pp.1–22, (2019)
11. Yang, Y., Gurbuz, O.D., Rebeiz, G.M.: An eight-element 370–410 GHz phased-array transmitter in 45-nm CMOS SOI with peak EIRP of 8–8.5 dBm. IEEE Trans. Microw. Theory Tech. **64**(12), 4241–4249 (2016)
12. Hertl, I., Vavrda, M., Hanulak, P.: Rotman lens design for millimeter-wave sensor application. In: IEEE Proceedings of 21st International Conference Radioelektronika, Brno, Czech Republic, 19–20 April 2011, pp. 1–4
13. Idrus, I.I., LatefI, T.A., Aridas, N.K., Talip, M.S.A., Yamada, Y., Rahman, T.A., Adam, I., Yasin, M. N. M.: A low-loss and compact single-layer butler matrix for a 5G base station antenna. PLoS ONE J, pp. 1–23, (2019)
14. Müller, D., Diebold, S., Reiss, S., Massler, H., Tessmann, A., Leuther, A., Zwick, T., Kallfass, I.: D-band digital phase shifters for phased-array applications. In: IEEE German Microwave Conference (GeMiC 2015), Nuremberg, Germany, 16–18 March 2015, pp. 205–208
15. He, Z.S., An, S., Liu, J., Jin, C.: Variable high precision wide D-band phase shifter. IEEE Access **8**, 140438–140444 (2020)
16. Nissanov (Nissan), U., Singh, G., Segun, A.: Sixth-generation (6G) microstrip antenna with high-gain. Int. J. Commun. Antenna and Propag. (IRECAP) **11**(4), 279–287 (2021)
17. Zhang, Y., Vilenskiy, A.R., Ivashina, M.V.: W-band waveguide antenna elements for wideband and wide-scan array antenna applications for beyond 5G. In: IEEE 15th European Conference on Antennas and Propagation (EuCAP), Dusseldorf, Germany, 22–26 March 2021, pp. 1–6.
18. Lu, P., Steeg, M., Kolpatzeck, K., Dulme, S., Khani, B., Czylwik, A., Stohr, A.: Photonic assisted beam steering for millimeter-wave and THz antennas. In: IEEE Conference on Antenna Measurements & Applications (CAMA), Sweden, 3–6 Sept. 2018, pp. 1–4
19. Islam, M.M., Leino, M., Luomaniemi, R., Song, J., Valkonen, R., Ala-Laurinaho, J., Viikari, V.: E-band beam-steerable and scalable phased antenna array for 5G access point. Int. J. Antennas Propag. **2018**(4267053), 1–10 (2018)
20. Elkhouly, M., Holyoak, M.J., Hendry, D., Zierdt, M., Singh, A., Sayginer, M., Shahramian, S., Baeyens, Y.: D-band phased-array Tx and Rx front ends utilizing radio-on-glass technology. In: IEEE Radio Frequency Integrated Circuits Symposium (RFIC), Los Angeles, CA, USA, 4–6 Aug. 2020, pp. 1–4
21. Mantash, M., Denidni, T.A.: millimeter-wave beam-steering antenna array for 5G applications. In: IEEE 28th Annual International Symposium on Personal, Indoor, and Mobile Radio Communications (PIMRC), Montreal, QC, Canada, 8–13 Oct. 2017, pp. 1–3
22. Mujammami, E.H., Afifi, I., Sebak, A.B.: Optimum wideband high gain analog beamforming network for 5G applications. IEEE Access **7**, 52226–52237 (2019)
23. Ershadi, S.E., Keshtkar, A., Bayat, A., Abdelrahman, A.H., Xin, H.: Rotman lens design and optimization for 5G applications. Int. J. Microw. Wireless Technol. **10**(9), 1048–1057 (2018)
24. Rotman, W., Turner, R.: Wide-angle microwave lens for line source applications. IEEE Trans. Antennas Propag. **11**(6), 623–632 (1963)
25. Hansen, R.C.: Design trades for Rotman lenses. IEEE Trans. Antennas Propag. **39**(4), 464–472 (1991)
26. Pozar, D.M.: Microwave Engineering, 2nd edn. Wiley, New York (1998)